Enhancement of Thermal Properties of Al/MoO_3 Thermite by Electrostatic Spraying

Jialin Chen[a], Shutao Li[a*], Yeqing Chen[a], Jiaxing Song[b]

[a] Institute of Defense Engineering, AMS, PLA, Beijing, 100036, China.

[b] Xi'an Rare Metal Materials Research Institute Co., Ltd., Xi'an, 710016, China.

* *Corresponding author:list16@tsinghua.org.cn*

Abstract: To improve the thermal properties of thermite safely and stably, electrostatic spraying was used to prepare the Al/MoO_3 thermite. The Al/MoO_3 thermites were detected and characterized by scanning electron microscopy (SEM) and X-ray diffraction (XRD), and thermal decomposition experiments were carried out by differential scanning calorimetry (DSC). The heat release of the Al/MoO_3 thermite prepared by the electrostatic spray (1044 $J \cdot g^{-1}$) is significantly higher than that of the thermite prepared by the ultrasonic (692 $J \cdot g^{-1}$), which is due to more uniform dispersion between Al and MoO_3. The initial reaction temperature and activation energy (Ea) of the former keep it steady. Electrostatic spray ensures the safety and stability of the Al/MoO_3 thermite. This study provides a new idea for safely and stably improving the thermal properties of thermite by enhancing surface homogenization, which is of great significance for practical applications.

Keywords: Al/MoO_3 thermite; electrostatic spraying; thermal behavior; activation energy.

1. Introduction

Energetic Materials (EMs) are a class of compounds or mixtures that contain a high amount of stored chemical energy.[1, 2] These materials can release much heat violently during the reaction. The thermite stands out due to its excellent combustion efficiency, high energy-releasing rate and high reaction exothermic enthalpy, which catches the attention of researchers. Thermite has been widely used in gas generator,[3] welding,[4] ammunition destruction[5] and high-energy additives in propellants.[6, 7]

The thermite composed of metal oxide and metal powder possesses unique chemical properties, which mainly is ascribed to the nature of its components. Typically, the thermite composed of Al and Fe_2O_3 is used for railway welding.[8] In the selection of metal powder, Al has been used in various conventional explosives and propellants to increase energy and temperature due to the advantages of high unit density exotherm, high reactivity and non-toxicity of reaction products. For metal oxides, there are so many choices. Wang[9] has successfully prepared Al/Fe_2O_3 thermite by sol-gel method for exploring the thermite reaction rate. Wang[10] has synthesized Al/CuO thermite with core-shell structure through self-assembly method, and the result showed that it had a good exothermic performance. Song[11] has prepared Al/MnO_2 thermite as a destroyer. Experiments showed the Al/MnO_2 thermite generated a bright flame during the reaction, which could easily penetrate the steel target, indicating the

thermite had a good cutting performance. Wolenski[12] has engineered the composition and morphology of Al/MoO_3 particles in thermite, which could promote the enhancement of reaction and the adjustment of combustion behavior. The chemical and physical properties of MoO_3 make it versatile so it can be used in optical, electronic, catalytic, biological and energy.[13] Besides, previous studies showed the Al/MoO_3 thermite owned better ignition performance.[14]

The thermite reaction, a solid-state diffusion process, is enhanced by decreasing the distance between metals and metal oxides. In other words, by improving the preparation method of the thermite to make the structure of the thermite more uniform, the thermal performance of the thermite can be effectively improved. Gash[15] has proposed Al/Fe_2O_3 thermite through the sol-gel reaction of metal salt and propylene oxide precursor. The results showed the thermite shortens the distance between Fe_2O_3 and Al, and inhibits the generation of Al oxide film, making the reaction more sufficient. However, the success of the sol-gel method is affected by a variety of factors, some of which are difficult to control. Zheng[16] has used the magnetron sputtering method to study the Al/Mn_2O_3 thermal film for the first time. Although the thermite prepared by this method has good thermal properties and excellent energy retention properties, the preparation equipment is expensive, the process is complicated, and the preparation amount is small. Electrostatic spraying, as a new preparation

process, has been widely used to make the sample more uniform through the action of a strong electric field.[17, 18]

In this paper, nano-MoO_3 was fabricated by hydrothermal method. Then, Al/MoO_3 nano-thermite was prepared by electrostatic spraying method. Also, Al/MoO_3 nano-thermite was prepared by ultrasonic dispersion method as the control group. Scanning electron microscopy (SEM) and X-ray diffraction (XRD) were used to detect and characterize the samples, and differential scanning calorimetry (DSC) was used to conduct thermal decomposition experiments. Multi-scan rate thermal analysis experiments were carried out for Al/MoO_3 nano-thermite, and the activation energy (Ea) of Al/MoO_3 nano-thermite was calculated. Finally, the mechanism of improving the thermal properties of the Al/MoO_3 nano-thermite prepared by electrostatic spraying was preliminarily analyzed.

2. Methods

2.1 Materials

All the chemicals (analytical grade) were purchased from Shanghai Chemical Reagents Co. without further purification. The mean size of 80 nm Al nanoparticles and 50 nm MoO_3 nanoparticles, were designated by the manufacturer. Absolute ethanol with a purity of 99.7% was chosen as a solvent to disperse the nanoparticles.

2.2 Preparation of Nano-MoO_3

One of the most common procedures for synthesizing MoO_3 was

used.[19] The schematic diagram of the preparation process is shown in Fig. 1.

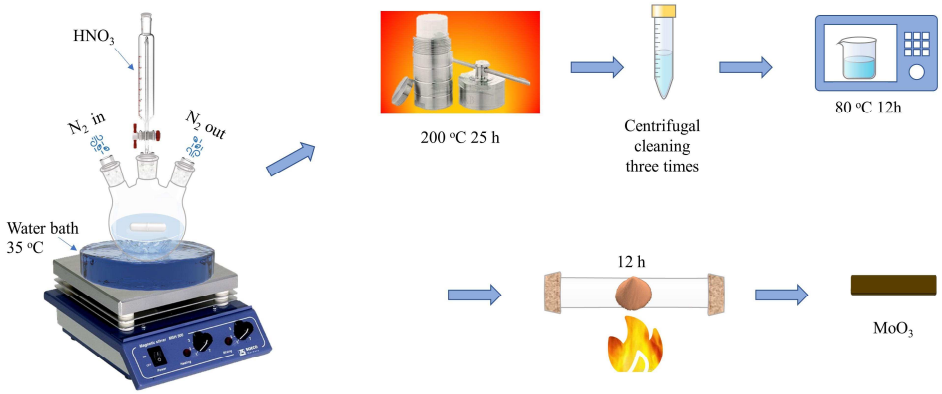

Fig.1 Schematic diagram of the preparation of nano- MoO_3

1.5 g of $(NH_4)_6Mo_7O_{24}\cdot 4H_2O$ and 30 mL of deionized water were poured into a beaker to prepare a certain concentration of ammonium molybdate solution, which was stirred strongly through a magnetic stirring device for 30 minutes. Then, 5 mL HNO_3 was extracted by pipette to dilute using 10 mL deionized water. Next, the diluted nitric acid solution was added dropwise to the stirring ammonium molybdate solution. At this time, white flocs were observed in the solution. The mixture solution was placed in the ultrasonic device at 25 °C for 10 minutes. Following this treatment, the solution was transferred into a 100 mL Teflon-lined steel stainless autoclave, sealed and kept at 200 °C for 25 hours. After the temperature of the autoclave was naturally returned to room temperature, the sample was then washed 3 times with deionized water and centrifuged. Later, the precipitate was dried at 80 °C for 12 hours. In the end, the sample was ground to place into a tube-type calciner, and baken at 400 °C for 12 hours

to obtain the MoO_3 sample. The chemical reaction equation is as follows.

$$Mo_7O_{24}^{6-} + 6H^+ \triangleq 7MoO_3 + 3H_2O \quad (1)$$

2.3 Nano-Al activity assay

Due to oxidation, the activity of nano-Al powder will not be 100%.[20] To analyze the content of active Al, the test was carried out by thermogravimetric analysis (TG) at 30 ~ 1200 °C with a heating rate of 10 $K \cdot min^{-1}$ and an airflow rate of 50 $mL \cdot min^{-1}$ to ensure complete oxidation of the nano-Al particles. The reaction of Al in air is as in Equation (2).

$$4Al + 3O_2 = 2Al_2O_3 \quad (2)$$

The TG analysis curve is shown in Fig. 2. Mass increase in the TG analysis is attributed to oxidation of active Al. The active Al content (c) can be calculated by Equation (3).

$$c(\%) = \frac{108}{96}\Delta m(\%) \quad (3)$$

Where, $\Delta m(\%)$ is the percentage of mass gain in TG analysis. It was concluded that the content of active Al is 65.5%.

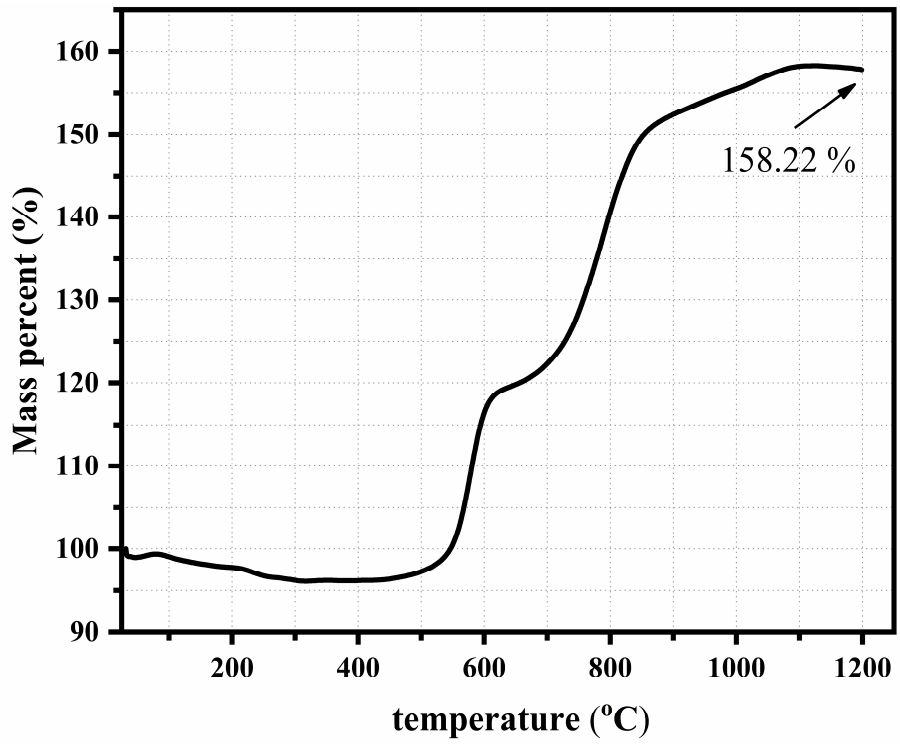

Fig.2 TG curve of nano-Al heated in air

2.4 Precursor preparation

Thermite samples were prepared using ultrasonic dispersion method. The mass of MoO_3 samples is controlled at 120 mg. According to the calculation of the chemical equation (4), the mass of fuel Al required for 120 mg of MoO_3 to reach zero oxygen balance is about 45 mg. However, the fuel used is only 65.5% active aluminum, so the mass of sample Al is 70 mg.

$$2Al + MoO_3 = Al_2O_3 + Mo \quad (4)$$

At first, 120 mg of nano-MoO_3 and 70 mg of nano-Al were respectively dispersed in absolute ethanol and magnetically stirred for 30 minutes. Then, two cups of solution were mixed into the same beaker and continued to be magnetically stirred for 20 minutes. Subsequently, the mixture was put into an ultrasonic cleaning machine and ultrasonically dispersed for 30 minutes to obtain a uniformly dispersed precursor suspension.

Two sets of solutions were prepared, one for subsequent electrostatic spray preparation of samples, labeled I. The other group was the control group, and the thermite sample was obtained by directly drying at 80 ^oC for 12 hours, which was marked as II.

2.5 Preparation of thermite by electrostatic spraying

The precursor solution was loaded into a syringe with a flat needle with a tip diameter of 0.42 mm. The syringe was pressurized through a

syringe pump and programmed to produce a spray rate of 4.0 $mL \cdot h^{-1}$. On the opposite side of the injector 10 cm, there was a square aluminum foil receiving plate with a length of 30 cm on one side, and a voltage of 13.5 kV was applied between the nozzle and the receiving plate. The ejected droplets formed a Taylor cone under the action of a strong voltage. The whole experiment was carried out in an environment with a relative humidity of 45%. The setup for the electrostatic spray experiment is shown in schematic Fig. 3.

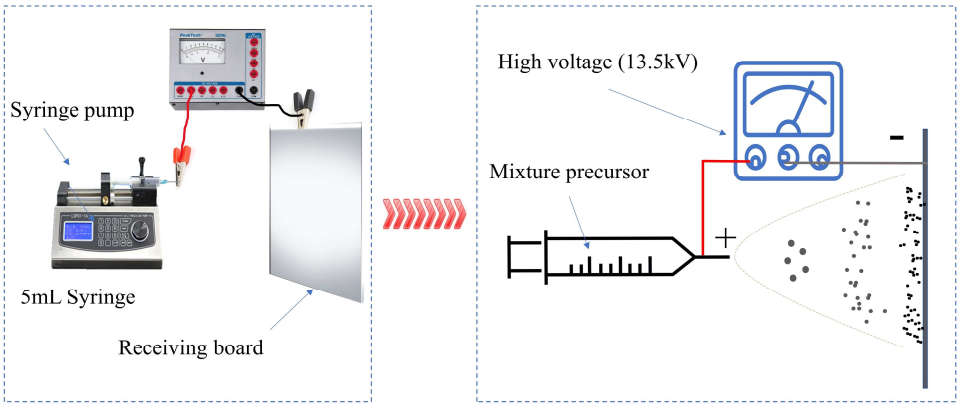

Fig.3 Schematic diagram of electrostatic spray experiment

The precursor liquid was ejected through the nozzle under the action of a strong electric field, and the nanoparticles attached to the charged droplet were accelerated by the electric field and formed a Taylor cone. Since the electrostatic force was greater than the molecular cohesion of the liquid, the ejected liquid was broken into a large number of small droplets.[18] At the same time, the solvent evaporated rapidly, leaving behind concentrated nano-solid particles that diffused onto the receiver plate to form a uniform, highly polymerized thermite composite.

Fig. 4 is the thermite powder formed by spraying on the aluminum

foil. A thin layer of film was formed on the surface of the aluminum foil, and the powder grew upright on the aluminum foil. The sediment was collected on the receiver plate with a spatula and placed in an antistatic bottle for later use.

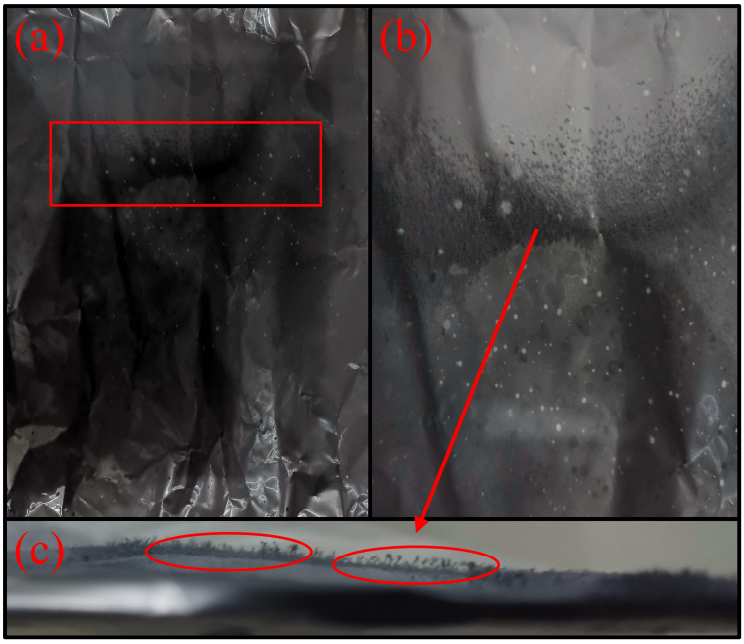

Fig.4 Electrostatic spray experiment effect

2.6 Characterization and thermal analysis

X-ray diffraction analysis (XRD, Bruker D8 Discover, Germany) was performed on the thermite samples to determine phase structures. The morphology of the samples was observed by scanning electron microscopy (SEM, JSM–7800F, Japan).

Thermogravimetric-differential scanning calorimetry (TG-DSC) method (NETZSCH STA 449F3, Germany) was introduced to measure the thermal properties of samples. The thermal analysis of thermites was conducted under the argon atmosphere with the temperature range from 40 ºC to 1000 ºC. Each sample was 3.0 mg for thermal safety, and the heating

rates was 15 K·min^{-1}. In the end, thermal analysis experiments are performed under different heating rates to determine the actuation energy (Ea). The heating rate were 10, 15, 20, 25 K·min^{-1}.

2.7 Theoretical analysis

The Kissinger method is one of the most well-known isoconversional methods on behalf of the differential method to determine Ea. The Ea of Al/MoO_3 thermite was obtained by using the Kissinger method. The Kissinger calculation method is shown in Equation 5.[21]

$$\ln\left(\frac{\beta}{T_P^2}\right) = \ln\frac{AR}{E_a} - \frac{E_a T_P}{R} \tag{5}$$

Where β is the linear heating rate (K·min^{-1}), T_P is the absolute temperature (K), R is the gas constant (J·mol^{-1}·K^{-1}), A is the pre-exponential factor (s^{-1}) and Ea is the activation energy (kJ·mol^{-1}).

Assuming that the reaction rate is maximized at the peak temperature, the plot of ln (β/T_P^2) vs. 1/T is a straight line, the slope of which is calculated as the value of the activation energy Ea.

3. Results and discussion

3.1 Microscopic morphology and crystal structure analysis

3.1.1 Microscopic morphology of synthetic MoO_3

Microscopic morphology and surface analysis of synthetic MoO_3 were observed by FE-SEM. In Fig. 5, SEM images show particles of synthetic samples adopt a rod morphology with diameters of 80 ~ 120 nm and lengths of 15 ~ 20 μm.

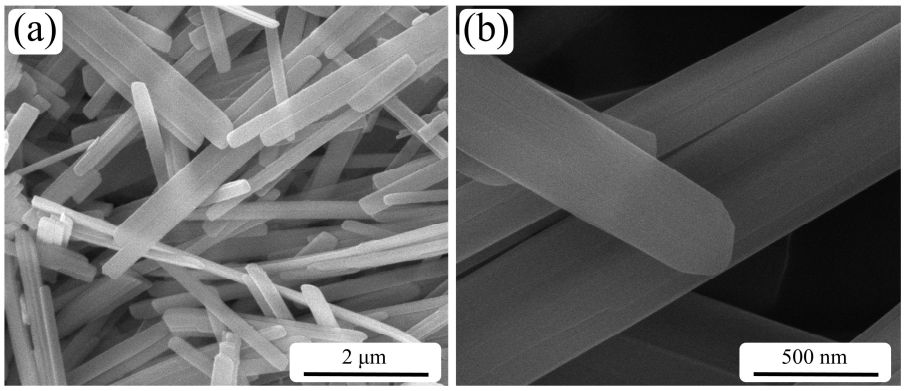

Fig.5 SEM image of nano-MoO_3

3.1.2 Crystal structures of synthetic MoO_3

To determine the crystal structures of obtained samples by hydrothermal method, XRD analysis was performed to test the phase structure. The results are shown in Fig. 6.

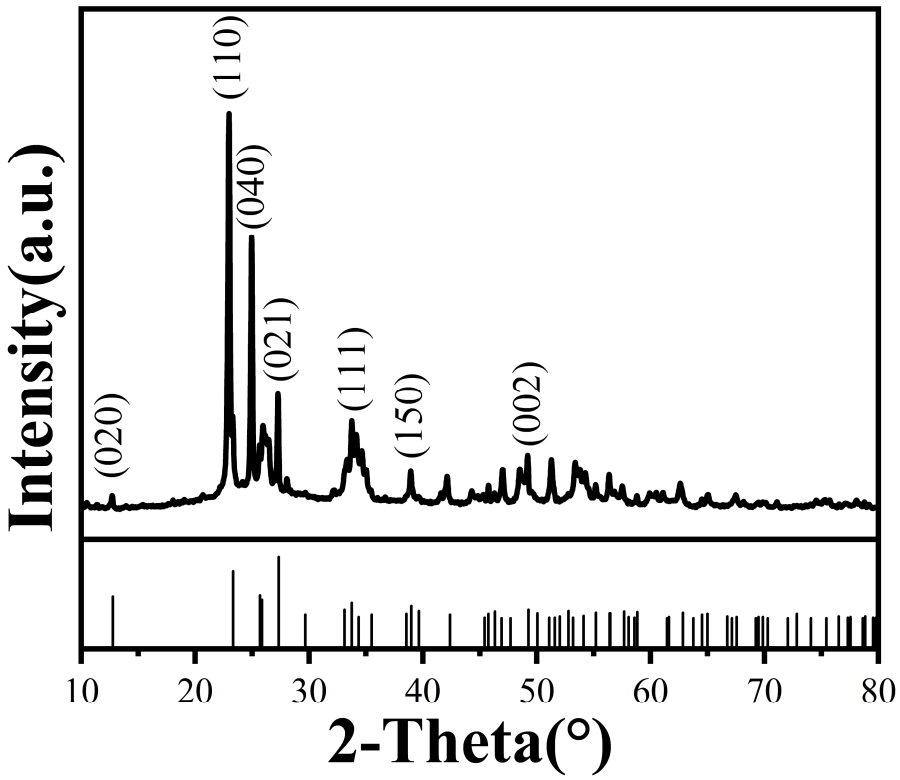

Fig.6 XRD curve of nano-MoO_3

Fig. 6 shows the diffraction peaks from 10° to 80°. The diffraction pattern for the samples has seven broad peaks at 12.8°, 23.3°, 25.7°, 27.3°, 39.0°, 49.3° and 58.8°, corresponding to (020), (110), (040), (021), (111),

(150) and (002), respectively. The XRD results show the synthesized sample is MoO_3, which provides evidence for subsequent research.

3.1.3 Crystal structures of thermite

The XRD patterns of the prepared I and II Al/MoO_3 thermites are shown in Fig. 7.

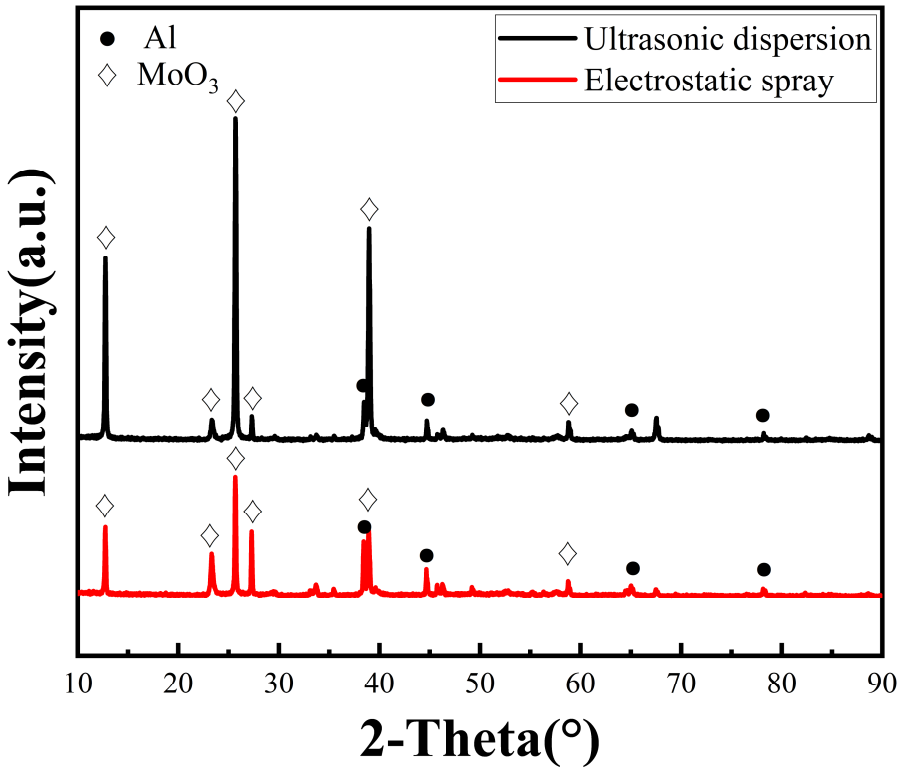

Fig.7 XRD curve of thermite

From the XRD curve, the diffraction peaks of MoO_3 (ICSD No. 89-7112 MDI Jade 6.0) and Al (ICSD No.04-0787 MDI Jade 6.0) can be retrieved. In addition, the diffraction peaks are sharp and intense, indicating that the prepared samples are highly crystalline and free of impurity peaks, confirming the high purity of the product.

3.1.4 Microscopic morphologies of thermite

To better observe the microscopic morphology, the thermite samples

I and II were observed using SEM. Fig. 8 (a) and (b) are the SEM images of the prepared thermite, in which the part selected by the red frame in the middle of the picture is individually enlarged for observing the distribution. There is an agglomeration of nano Al particles in Fig. 8 (a). Although part of Al is also agglomerated in Fig. 8 (b), more Al particles are evenly dispersed. The SEM images better illustrate the uniformity of the dispersion of the samples.

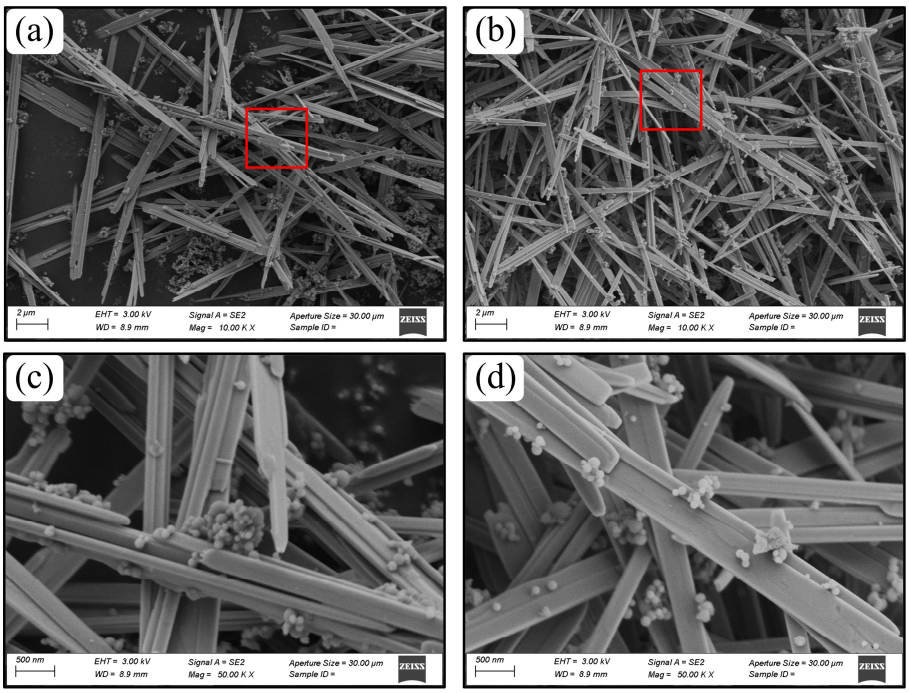

Fig.8 SEM image of thermite. (a) Al/MoO_3 thermite prepared by ultrasonic dispersion (b) Al/MoO_3 thermite prepared by Electrostatic spray (c) and (d) Enlarged image in the red box

To further analyze the dispersion of MoO_3 and Al in the thermite, SEM-Mapping characterization was carried out. Fig. 9 (a) shows Al has an obvious agglomeration phenomenon. In the red circle, Al accumulation occurs, and in the corresponding area, there is less MoO_3 distribution. By contrast, in Fig. 9 (b), The distribution of MoO_3 is in the shape of thin stripes MoO_3, Al is uniformly dispersed along its grain, which illustrates

Al and MoO_3 are well dispersibility.

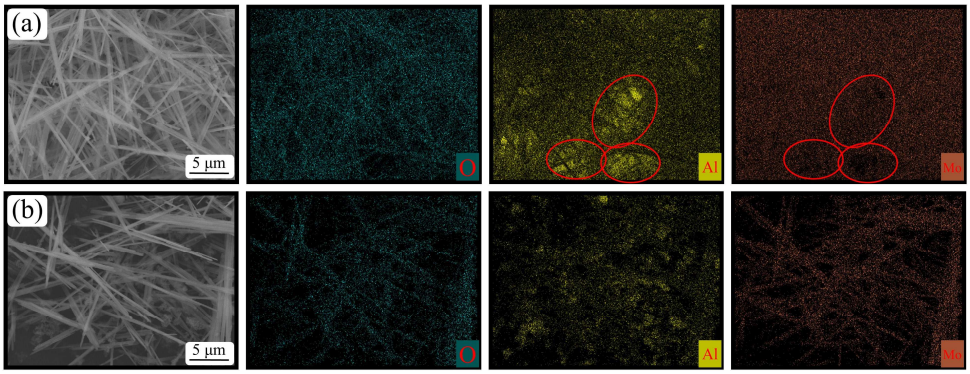

Fig.9 SEM-Mapping image of thermite. (a) Al/MoO_3 thermite prepared by ultrasonic dispersion (b) Al/MoO_3 thermite prepared by Electrostatic spray

3.2 Thermal analysis

The thermal properties of the thermite samples were tested by DSC, as shown in Fig. 10. The details of the main exothermic peaks of the thermite samples are listed in Table 1.

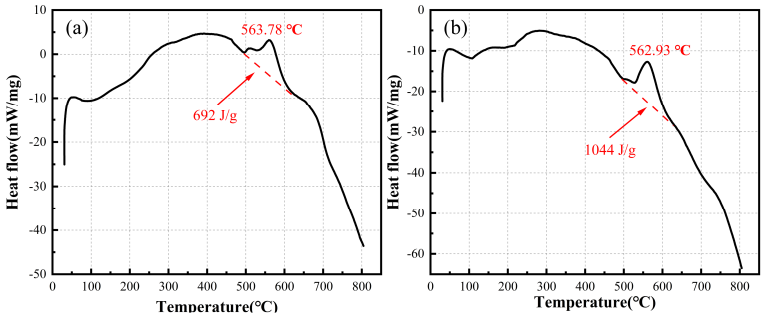

Fig.10 DSC curve of thermite. (a) Al/MoO_3 thermite prepared by ultrasonic dispersion (b) Al/MoO_3 thermite prepared by Electrostatic spray

Fig. 10 (b) shows the DSC image curve of the Al/MoO_3 thermite prepared by the electrostatic spray method is consistent with the overall trend of the DSC curve of that prepared by the ultrasonic dispersion method. There is only a significant difference in the heat release. The Al/MoO_3 thermite prepared by ultrasonic dispersion has an obvious exothermic peak at 563.78 °C, and the exotherm is 692 $J \cdot g^{-1}$. The exothermic heat of

Al/MoO_3 thermite prepared by electrostatic spraying increased obviously, which is 1044 $J \cdot g^{-1}$. At the same time, the initial exothermic temperature of the Al/MoO_3 thermite prepared by the electrostatic spray method is relatively stable. Compared with the Al/MoO_3 thermite prepared by the ultrasonic dispersion method, there is no major change, which ensures safety and does not release heat prematurely.

Table 1 Details of the main exothermic peaks of nano-thermite

Sample	Initial reaction temperature (°C)	Peak temperature (°C)	Heat release ($J \cdot g^{-1}$)
I	534	563	692
II	529	562	1044

The thermal properties of the Al/MoO_3 thermite prepared by electrostatic spraying are significantly improved, benefiting from its more uniformly dispersed structure. As shown in Fig. 9 (b), Al is distributed along the shape of MoO_3 thin rods and is relatively uniform. On the contrary, in the Al/MoO_3 thermite prepared by the ultrasonic dispersion method, the distribution of Al is not uniform, and there is a relatively obvious agglomeration phenomenon. Its reaction mechanism is shown in Fig. 11. The contact area of the agglomerated Al and MoO_3 is small, so the effective area of the aluminothermic reaction is small. In sample I, the contact area between Al and MoO_3 is larger, which is conducive to the more complete reaction, so the heat released by the reaction is more[22].

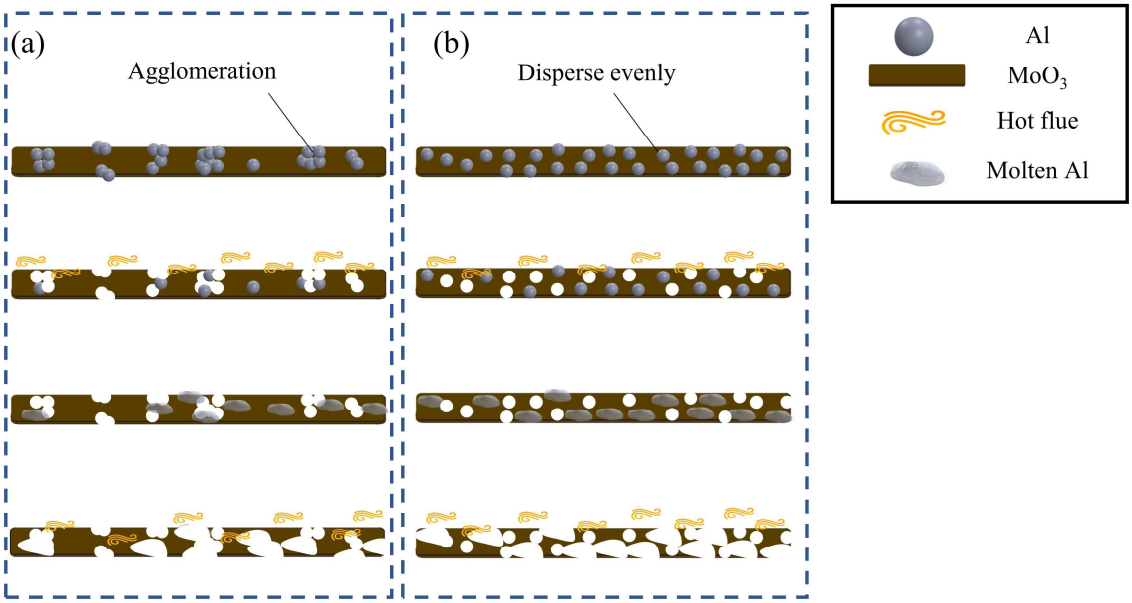

Fig. 11 Schematic diagram of the reaction mechanism of the $AlMoO_3$ thermite heating process

3.3 Non-isothermal thermodynamic analysis

To explore the thermal kinetics of the Al/MoO_3 thermite, DSC analysis experiment of multiple heating rates was carried out, which could obtain the Ea of the sample. Ea is an indicator of the minimum energy required for a chemical reaction, and it can reflect the difficulty of the chemical reaction.[23]

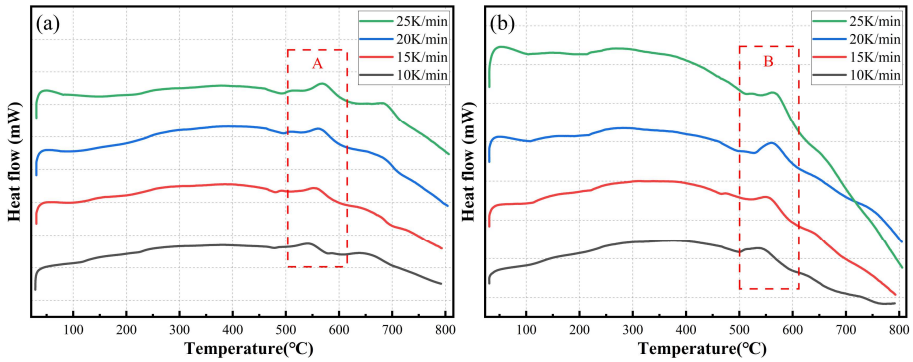

Fig. 12 the curves of 4 groups of DSC. (a) Al/MoO_3 thermite prepared by ultrasonic dispersion (b) Al/MoO_3 thermite prepared by Electrostatic spray

The thermal kinetics of the Al/MoO_3 thermite were obtained through Equation 5. The detail of calculation parameters of Ea for sample thermite reaction is shown in Table 2. The linear fitting diagram of the peak

temperature point of the sample DSC test is shown in Fig. 13.

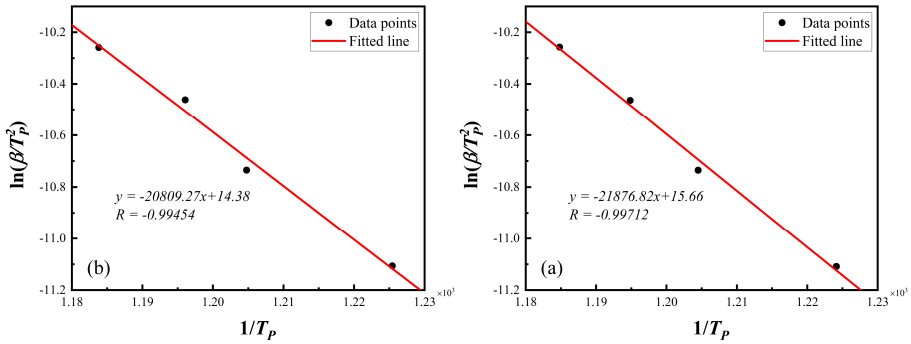

Fig. 13 Activation energy of Al/MoO_3 thermite. (a) Al/MoO_3 thermite prepared by ultrasonic dispersion (b) Al/MoO_3 thermite prepared by Electrostatic spray

Fig. 13 (a) shows the straight line fitted by sample I is $y = -21876..8x + 15.7$, the Ea is 181.88 kJ·mol^{-1} by calculation. The R is 0.99712, indicating a high degree of fitting. The straight line fitted by sample II is $y = -20809.2x + 14.4$, R is 0.99454, and the obtained Ea is 173.01 kJ·mol^{-1}, which is a bit smaller than sample I. This further illustrates the stability and safety of the Al/MoO_3 thermite prepared by the electrostatic spray method and will not be excited to release heat prematurely. Under the premise of ensuring safety and stability, the Al/MoO_3 thermite prepared by the electrostatic spray method has greatly improved the heat release and its thermal performance has been significantly improved.

Table 2 Exothermic peak data table of 4 groups of DSC curves of nano-thermite

Sample	Peak temperature （℃）	Peak temperature (K)	Heating rate (K/min)	$1/T$	ln (β/T_P^2)
I	543	816	10	0.00122414	-11.10844828
	557	830	15	0.0012045	-10.73533125
	563	836	20	0.001194843	-10.4637486
	570	844	25	0.001184806	-10.25747656
II	542	816	10	0.00122543	-11.10634165
	556	830	15	0.001204776	-10.73487349
	562	836	20	0.001196058	-10.46171633
	571	844	25	0.001183824	-10.2591346

4. Conclusion

The MoO_3 was prepared via the hydrothermal process, and then Al/MoO_3 thermite was prepared by electrospray. At the same time, Al/MoO_3 thermite was prepared by ultrasonic dispersion method as a control group. SEM, XRD, and DSC were carried out to explore their thermal properties.

DSC analysis showed the thermal decomposition performance of Al/MoO_3 thermite prepared by electrospray was better than Al/MoO_3 thermite prepared by ultrasonic dispersion method, which was manifested in the fact that the released heat of the former thermite, 1044 J g^{-1} was more than 692 J g^{-1} of the latter thermite. The obvious improvement in thermal properties of Al/MoO_3 thermite prepared by electrostatic spraying is due to its more uniformly dispersed structure.

Neither the initial reaction temperature of thermite nor the Ea obtained by non-isothermal thermodynamic analysis has a significant decrease. It shows Al/MoO_3 thermite prepared by electrospray presents good thermal stability, will not be easily excited, premature thermal decomposition, which ensures safety.

In a word, the thermal properties of the thermite prepared by the electrostatic spray method have been greatly improved, and the safety is ensured, laying a foundation for the subsequent scientific research technology and product manufacturing application.

5. Conflicts of interest

The authors declare that there is no conflict of interest regarding the publication of this paper.

6. Acknowledgments

It was performed using the equipment at the School of Chemical Engineering at Nanjing University of Science and Technology (NUST).

7. References

1. Wang Q, Xing B, Guo X, Bao H, Wang Y, Li A, et al. Facile preparation of Si/CuO energetic materials by electrophoretic deposition and their exothermic studies. Vacuum. 2019;167:244-8.

2. Ke X, Zhou X, Hao G, Xiao L, Liu J, Jiang W. Rapid fabrication of superhydrophobic Al/Fe_2O_3 nanothermite film with excellent energy-release characteristics and long-term storage stability. Applied Surface Science. 2017;407:137-44.

3. Wu T, Sevely F, Julien B, Sodre F, Cure J, Tenailleau C, et al. New coordination complexes-based gas-generating energetic composites. Combustion and Flame. 2020;219:478-87.

4. Josefson BL, Bisschop R, Messaadi M, Hantusch J. Residual stresses in thermite welded rails: significance of additional forging. Welding in the World. 2020;64(7):1195-212.

5. Chen J, Guo T, Song J, Yao M, Ding W, Liu X, et al. The characteristics of combustion reactions involving thermite under different shell materials. RSC advances. 2020;10(56):33762-9.

6. Ryan Bratton K, Hill KJ, Woodruff C, Cagle C, Pantoya ML, Abraham J, et al. Tailoring impact debris dispersion using intact or fragmented thermite projectiles. Journal of Applied Physics. 2020;128(15):155108.

7. Wang J, Chen S, Wang W, Zhao F, Xu K. Energetic properties of new nanothermites based on in situ $MgWO_4$-rGO, $CoWO_4$-rGO and Bi_2WO_6-rGO. Chemical Engineering Journal. 2022;431.

8. Lee S, Kim J, Lee C. Reactivity Enhancement and Fabrication of Al-MoO_3 Thermite Coating Using Ball Milling for Kinetic Spraying. Journal of Thermal Spray Technology. 2020;29(7):1669-81.

9. Yi W, Song X-l, Jiang W, Deng G-d, Guo X-d, Liu H-y, et al. Mechanism for thermite reactions of aluminum/iron-oxide nanocomposites based on residue analysis. Transactions of Nonferrous Metals Society of China. 2014;24(1):263-70.

10. Wang Q, Ma Y, Wang Y, Bao H, Li A, Xu P, et al. Facile fabrication of highly exothermic CuO@Al nanothermites via self-assembly approach. Nanotechnology. 2019;31(5):055601.

11. Song J, Fang X, Guo T, Ding W, Yao M, Zhang X, et al. Thermal Reaction Processes and Characteristics of an Al/MnO_2 Pyrotechnic Cutting Agent Based on Residuel Analyses. Materiali in tehnologije. 2020;54(3):327-33.

12. Wolenski C, Wood A, Mathai CJ, He X, McFarland J, Gangopadhyay K, et al. Nanoscale surface reactions by laser irradiation of Al nanoparticles on MoO_3 flakes. Nanotechnology. 2018;30(4):045703.

13. Castro D, Alves I, Datta, Shankar R, Zhen J, Castellanos-Gomez, et al. Molybdenum Oxides - From Fundamentals to Functionality. Advanced Materials. 2017;29(40):1701619.

14. Sun J, Pantoya ML, Simon SL. Dependence of size and size distribution on reactivity of aluminum nanoparticles in reactions with oxygen and MoO_3. Thermochimica Acta. 2006;444(2):117-27.
15. Tillotson T, Gash A, Simpson R, Hrubesh L, Satcher Jr J, Poco J. Nanostructured energetic materials using sol–gel methodologies. Journal of Non-Crystalline Solids. 2001;285(1-3):338-45.
16. Zheng G, Zhang W, Shen R, Ye J, Qin Z, Chao Y. Three-dimensionally ordered macroporous structure enabled nanothermite membrane of Mn_2O_3/Al. Scientific reports. 2016;6(1):1-10.
17. Wang W, Li H, Yang Y, Zhao F, Li H, Xu K. Enhanced thermal decomposition, laser ignition and combustion properties of NC/Al/RDX composite fibers fabricated by electrospinning. Cellulose. 2021;28(10):6089-105.
18. Song J, Guo T, Ding W, Yao M, Bei F, Zhang X, et al. Study on thermal behavior and kinetics of Al/MnO_2 poly (vinylidene fluorine) energetic nanocomposite assembled by electrospray. RSC advances. 2019;9(44):25266-73.
19. Hu X, Xiao L, Jian X, Zhou W. Integration of nano-Al with one-step synthesis of MoO_3 nanobelts to realize high exothermic nanothermite. Science Engineering of Composite Materials. 2018;25(3):579-85.
20. Zhou X, Zhu Y, Ke X, Zhang K. Exploring the solid-state interfacial reaction of Al/Fe_2O_3 nanothermites by thermal analysis. Journal of Materials Science. 2019;54(5):4115-23.
21. Kissinger HE, editor Reaction Kinetics in Differential Thermal Analysis1957.
22. Egan GC, Zachariah MR. Commentary on the heat transfer mechanisms controlling propagation in nanothermites. Combustion and Flame. 2015;162(7):2959-61.
23. Lv J, Chen L, Chen W, Gao H, Peng M. Kinetic analysis and self-accelerating decomposition temperature (SADT) of dicumyl peroxide. Thermochimica acta. 2013;571:60-3.